Molecular Crystals and Liquid Crystals

ISSN: 1542-1406 (Print) 1563-5287 (Online) Journal homepage: http://www.tandfonline.com/loi/gmcl20

Characterization of PDPA-b-PDMA-b-PDPA triblock copolymer Langmuir-Blodgett films for organic vapor sensing application

Y. Acikbas, F. Taktak, C. Tuncer, V. Bütün, R. Capan & M. Erdogan

To cite this article: Y. Acikbas, F. Taktak, C. Tuncer, V. Bütün, R. Capan & M. Erdogan (2016) Characterization of PDPA-b-PDMA-b-PDPA triblock copolymer Langmuir-Blodgett films for organic vapor sensing application, Molecular Crystals and Liquid Crystals, 634:1, 104-117, DOI: 10.1080/15421406.2016.1177911

To link to this article: http://dx.doi.org/10.1080/15421406.2016.1177911

MOLECULAR CRYSTALS AND LIQUID CRYSTALS
2016, VOL. 634, 104–117
http://dx.doi.org/10.1080/15421406.2016.1177911

Taylor & Francis
Taylor & Francis Group

Characterization of PDPA-*b*-PDMA-*b*-PDPA triblock copolymer Langmuir-Blodgett films for organic vapor sensing application

Y. Acikbas[a], F. Taktak[b], C. Tuncer[c], V. Bütün[c], R. Capan[d], and M. Erdogan[d]

[a]Department of Material Science and Nanotechnology Engineering, Faculty of Engineering, University of Usak, Usak, Turkey; [b]Department of Chemical Engineering, Faculty of Engineering, University of Usak, Usak, Turkey; [c]Department of Chemistry, Faculty of Arts and Science, University of Eskişehir Osmangazi, Eskişehir, Turkey; [d]Department of Physics, Faculty of Science, University of Balikesir, Balikesir, Turkey

ABSTRACT

This study reports the synthesis, characterization, and gas sensing applications of the PDPA-*b*-PDMA-*b*-PDPA triblock copolymer material using NMR, UV-visible spectroscopy, atomic force microscopy (AFM), quartz crystal microbalance (QCM), and Langmuir-Blodgett (LB) thin film deposition techniques. The thin film deposition conditions of the copolymer material, which are prepared by LB film technique, are characterized by UV-visible spectroscopy, AFM, and QCM system. In this study, the swelling behaviors of the PDPA-*b*-PDMA-*b*-PDPA triblock copolymer Langmuir-Blodgett (LB) films were investigated with respect to volatile organic compounds (VOCs) at room temperature. The sensing responses of the films against VOCs were measured by QCM method. The swelling processes could be investigated using the early-time Fick's law of diffusion.

KEYWORDS

Copolymers; Diffusion; Langmuir-Blodgett films; QCM; Sensors; Swelling

Introduction

Polymers and their derivatives have been attracting the attention and interest of researchers in many fields because of their remarkable properties leading to potential applications in life sciences [1], drug delivery systems [2], solar cells [3], organic electronic materials [4], and chemical sensors [5]. For the development of chemical sensors (devices for detecting gases and volatile organic compounds (VOCs)), these materials promise reduced cost, higher portability, and operation at low power and as a result have actually received considerable attention. Polymeric materials are commonly utilized as responsive coatings in chemical sensors due to their capability to absorb a variety of different molecules. Due to their flexible chains, the molecules can easily be absorbed into polymer materials. This absorption process leads to swelling, which results from the mass increase of the polymer materials [6, 7]. Several measurement techniques such as ellipsometry, spectroscopy, interferometry, surface plasmon resonance, or quartz crystal microbalance (QCM) techniques can be used to detect these chemical sensors due to their potential applications [8–11]. Among these techniques, QCM has recently been prefered in chemical gas sensor applications [12–14].

In this work, the PDPA-*b*-PDMA-*b*-PDPA triblock copolymer was selected as potential sensor material due to little information in the available literature on the investigation of the

CONTACT F. Taktak fulya.taktak@usak.edu.tr
Color versions of one or more of the figures in the article can be found online at www.tandfonline.com/gmcl.

swelling behaviors of the triblock copolymer Langmuir-Blodgett (LB) thin film using QCM technique. To study the swelling mechanism in sensor applications, LB films were subjected to the saturated VOCs' vapors. The frequency shift of the quartz resonators was recorded as a function of time during swelling resulting from the bulk diffusion process. The diffusion coefficients (D) of VOCs could be calculated by using early-time Fick's law of diffusion, adopted to fit the QCM results.

Experimental details

The synthesis of the PDPA-*b*-PDMA-*b*-PDPA triblock copolymer was realized by using group transfer chemistry [15]. Typically, tetra-*n*-butylammonium bibenzoate catalyst (approximately 100 mg) was added from a side arm under a nitrogen atmosphere into a 250 mL triple neck round-bottom flask. After transferring both tetrahydrofuran (125 mL) and 1-methoxy-1-trimethylsiloxy-2-methyl-1-propene (0.23 mL) into the flask via cannula, the solution was stirred and then first monomer (DPA, 2-(diisopropylamino)ethyl methacrylate, 5.0 mL) was added. During this first polymerization, an exotherm was monitored with a contact thermocouple attached to the side of the flask. It was noticed that the reaction temperature increased by 4 °C. After polymerization mixture was cooled *back* down to *room temperature*, a 2 mL aliquot was extracted via syringe for gel permeation chromatography (GPC) and proton NMR analysis. Then, the second monomer, 2-(dimethylamino)ethyl methacrylate (DMA, 20.0 mL), was added and a second exotherm was recorded. The reaction mixture was stirred and allowed to cool to room temperature (approximately 50 min). Finally, to produce an ABA triblock copolymer (PDPA-*b*-PDMA-*b*-PDPA), after extraction of a small aliquot from the polymerizing PDPA-*b*-PDMA reaction mixture, the third monomer (DPA, 5.0 mL) was added via cannula. The reaction mixture was allowed to *reach to room temperature* (approximately 50 min). After aliquot extraction for GPC analysis, the reaction was quenched by adding a small amount of methanol (2 mL) prior to recovery using a rotary evaporator. The resulting triblock copolymer was dried on a vacuum line overnight after removing PDPA and PDPA-*b*-PDMA contaminations by using cold hexane. The actual DP's of the final PDPA-*b*-PDMA-*b*-PDPA triblock copolymer were calculated from ^{1}H NMR spectra as being 19, 71, and 10, respectively (Fig. 1). GPC analysis showed $M_n = 37{,}800$ and $M_w/M_n = 1.05$.

PDPA-*b*-PDMA-*b*-PDPA triblock copolymer could be dissolved in chloroform with a ratio of concentration approximately 0.32 mg mL^{-1}. This solution was used to take an isotherm and to produce an LB film by spreading it on the distilled water surface. Before the isotherm graph was taken, 15 min was allowed for the solvent to evaporate. The isotherms were recorded with the compression speed of 30 cm^2 min^{-1} at pH 6.0. The isotherm graph was repeated several times and the results were found to be reproducible at room temperature. In this study, the deposition pressure and deposition mode were 13.8 mN m^{-1} and *Z*-type, respectively.

Figure 2 shows a block diagram of our home-made QCM measurement system. A thinly cut wafer of raw quartz sandwiched between two electrodes in an overlapping keyhole design was used for the QCM measurement. AT-cut quartz crystals with a resonant frequency of 3.5 MHz were commercialized from GTE SYLVANIA company. All measurements were taken at room temperature (20°C) using an oscillating circuit designed in-house. At the beginning of the measurement, a clean quartz crystal was inserted into the electronic unit, and the quartz crystal was placed in a gas chamber. In order to obtain f_0, which is the resonant frequency of noncoated quartz crystal, the frequency shift of quartz crystal was measured, and the frequency response was stable within ± 1 Hz over a period of 30–45 min. After each deposition cycle, the LB film sample was dried for half an hour and the mass change was monitored using

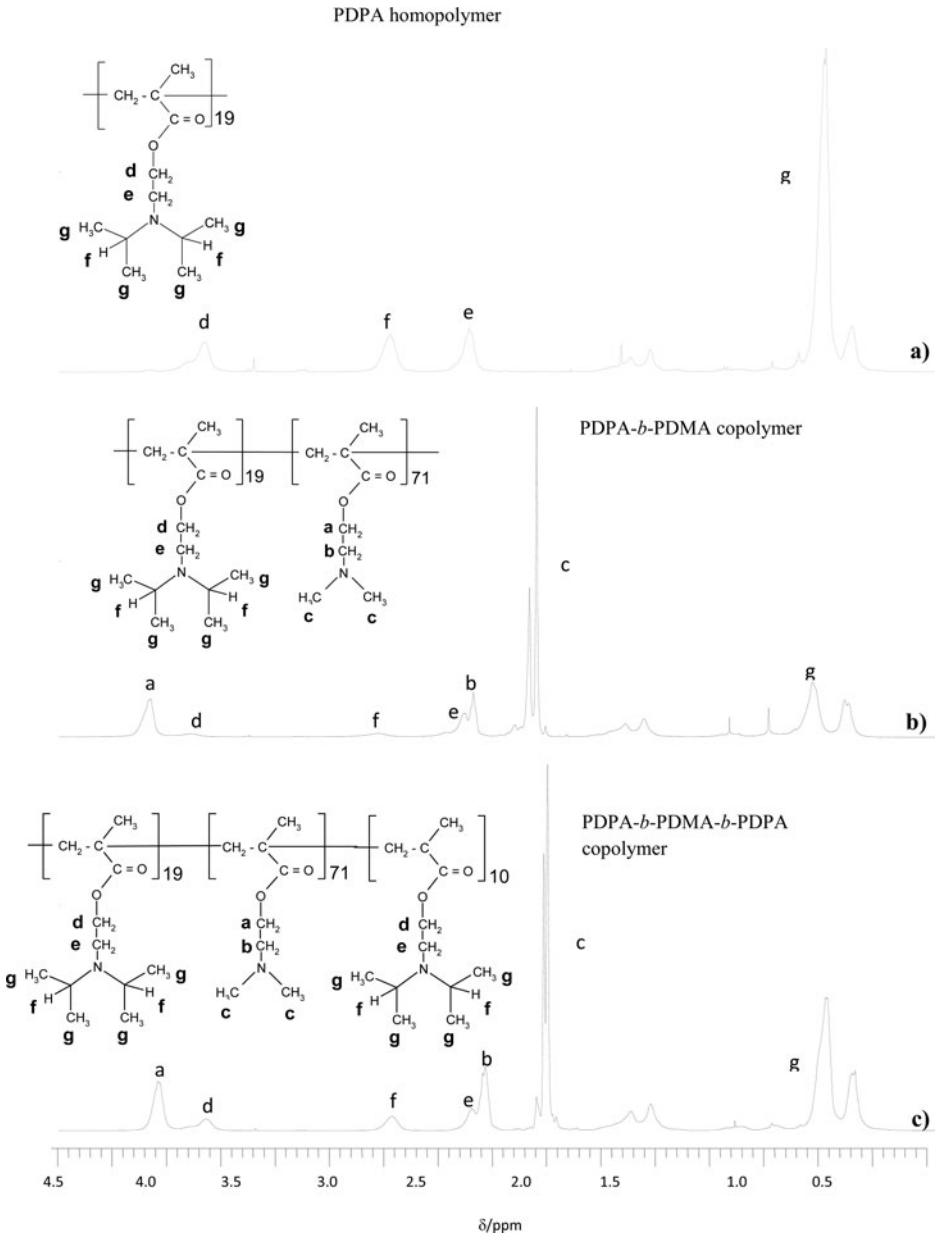

Figure 1. Proton NMR spectra in $CDCl_3$: (a) PDPA homopolymer (before addition of DMA and DPA monomers); (b) PDPA-*b*-PDMA diblock copolymer; and (c) PDPA-*b*-PDMA-*b*- PDPA triblock copolymer.

this computer controlled QCM measurement system. This system was used for the confirmation of the reproducibility of LB film multilayers using the relationship between the QCM frequency changes against the deposited mass, which should depend on the number of layers in the LB film.

A gas cell was constructed to study the LB film response on exposure to organic vapors by measuring the frequency change and these measurements were performed with a syringe. The sample was periodically exposed to organic vapors at least for 2 min, and was then allowed to recover after injection of dry air. The changes in resonance frequency were recorded in real

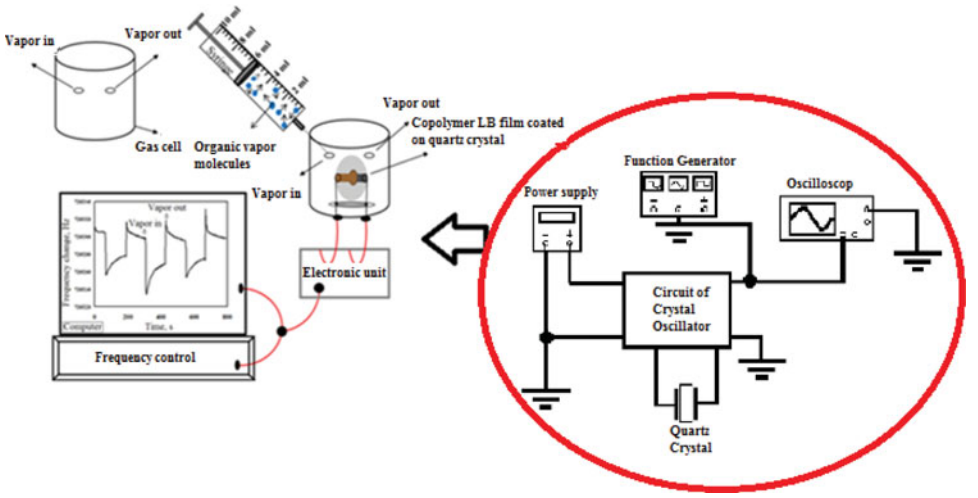

Figure 2. A block diagram of the quartz crystal microbalance measurement system.

time during exposure to organic vapors. This procedure was carried out over several cycles to observe the reproducibility of the LB film sensing element.

Result and discussion

Isotherm properties and transfer ratio

Figure 3 shows the isotherm graphs of the PDPA-*b*-PDMA-*b*-PDPA triblock copolymer for $V = 100\mu\ l$, $V = 200\mu\ l$, and $V = 300\mu\ l$ (V is the volume of solution spread over the water surface). The suitable surface pressure for this copolymer LB film deposition procedure was selected as 13.8 mN m^{-1}.

The transfer ratio for a Langmuir-Blodgett thin film deposition is also an important parameter to monitor the deposition process. It is defined as the ratio of the area of the

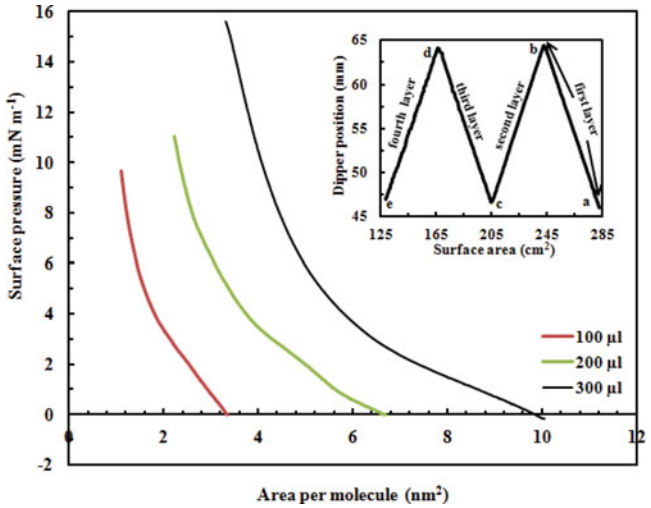

Figure 3. Isotherm graphs of the copolymer monolayer. Inset: The number of LB deposition cycles of the copolymer thin film onto quartz glass substrate.

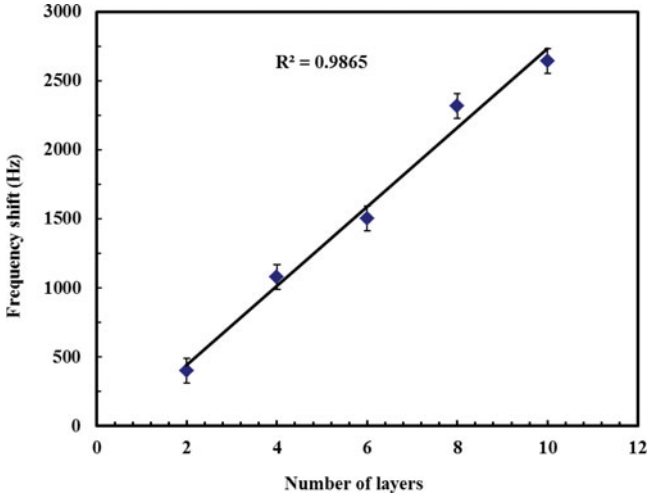

Figure 4. Frequency changes as a function of copolymer LB film layer numbers.

Langmuir-Blodgett film removed from the water surface to the area of the substrate moved through the air-monolayer-water surface.

$$TR = A_1/A_2, \tag{1}$$

where A_1 is the occupied area by the monolayer on the water surface, and A_2 is the deposited area of the quartz crystal or quartz glass substrate. The reduced surface area change of the copolymer monolayers during the deposition onto a quartz glass substrate for four bilayers is given in the inset in Fig. 3. The labels of the inset in Fig. 3 are pointed from position (a) to position (b) right-to-left direction when the first LB film layer deposited onto the quartz glass substrate. Similar labeling is made for the second, third, and fourth layers. It is found that the average reduction of the area for each bilayer was almost the same during the deposition process of monolayers onto the quartz glass substrate. Transfer ratio values are calculated using Equation (1), and these values are obtained over 92% for the PDPA-*b*-PDMA-*b*-PDPA triblock copolymer molecules. These results display that these copolymer molecules can be deposited onto solid substrates successfully with remarkably transfer ratios. Similar results are observed in studies on octadecyl trimethyl ammonium bromide (OTAB) and polymeric nonionic photoacid generator (PAG) copolymer, where transfer ratios were found to be 0.98 and 0.90, respectively [16, 17].

QCM and UV-visible measurements

QCM system is fairly sensitive to a small mass change at a nanoscale, which is used for measuring the resonance frequency of quartz crystal. The resonance frequency change (Δf) on LB film multilayer quartz crystal against a mass change per unit area (Δm) is given by [18]

$$\Delta f = -\left(2 f_0^2 \Delta m/{\rho_q}^{1/2} {\mu_q}^{1/2} A\right) N, \tag{2}$$

where Δf is the frequency change (Hz), f_0 is the resonant frequency of noncoated quartz crystal (Hz), Δm is the deposited mass per unit area per layer (g), ρ_q is the density of quartz (2.648 g cm^{-3}), μ_q is the shear modulus of quartz (2.947 $\times$ 10^{11} g cm^{-1} s^{-2}), A is the electrode active area (2.65 cm^2), and N is the number of deposited LB film layers.

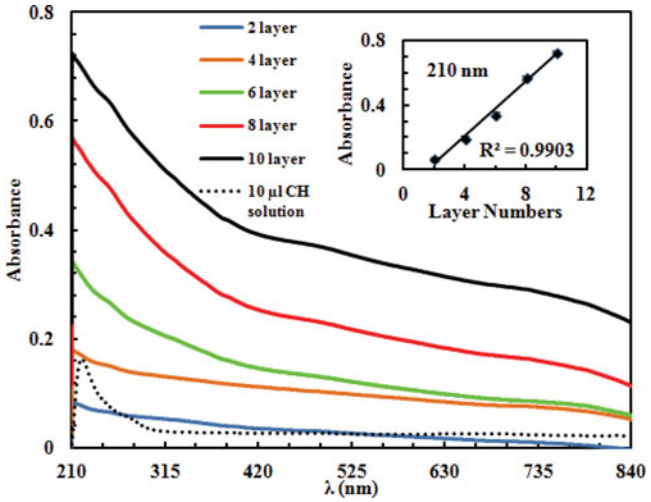

Figure 5. UV-vis spectras of the copolymer in a chloroform solution and the copolymer LB film on the quartz glass. Inset: Linear increase of absorbance as a function of layer numbers.

Figure 4 describes the deposition of the copolymer LB films onto quartz resonators for 10 layers. The change in resonance frequency as a function of the number of monolayers is closely associated with the LB layer mass change. A linear dependence reveals that equal mass per unit area is deposited onto the quartz crystal during the deposition of LB film layers. The frequency shifts of 286.15 Hz per layer for the copolymer LB films are obtained from the curve of the plot. The mass deposited on the quartz crystal per bilayer is estimated as 3893.15 ng (14.69 ng mm^{-2}) for the copolymer LB film using Equation (2) and Fig. 4.

Figure 5 displays both the UV-vis absorption spectra of a PDPA-*b*-PDMA-*b*-PDPA triblock copolymer solution in chloroform and PDPA-*b*-PDMA-*b*-PDPA triblock copolymer LB films transferred onto a quartz glass substrate with different layer thicknesses. The UV-vis spectrum of the PDPA-*b*-PDMA-*b*-PDPA triblock copolymer solution is observed at around 220 nm. Figure 5 also shows the absorption spectra, at 210 nm, for 2–10 layers of the PDPA-*b*-PDMA-*b*-PDPA triblock copolymer LB films on the quartz glass substrate. The UV-vis spectra of the LB films are similar to the solution spectra but the band at 210 nm is broadened in the solution spectrum and is blue shifted by about 10 nm. The shift in the absorption band of the LB film may be the result of some kind of molecular aggregation occurring during film formation. In order to monitor the deposition of LB film layer onto the quartz substrate, the relationship between the absorbance and layer numbers is investigated. The inset in Fig. 5 shows a plot of the absorption intensity at 210 nm relative to the layer numbers of LB films, which reveal an almost linear increase of the absorption intensity with the layer numbers. The linear relationship between the absorbance and the number of layers suggests that a regular deposition of the PDPA-*b*-PDMA-*b*-PDPA triblock copolymer monolayer takes place, resulting in fairly uniform LB films. This means that similar amount of the PDPA-*b*-PDMA-*b*-PDPA triblock copolymer is transferred during each LB deposition. Similar linear relationships are obtained with plots of the absorbance at 225 nm for PAG-copolymer LB films [17] and at 193 nm for p(DDA-*t*BVPC53) LB films [19].

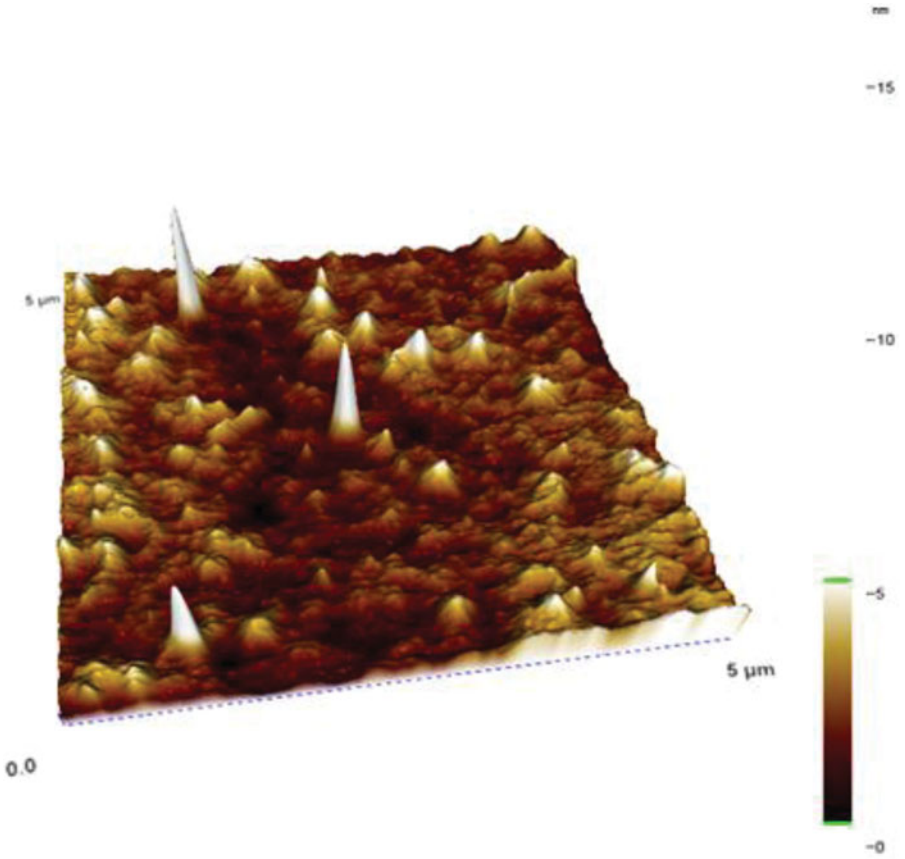

Figure 6. Three-dimensional AFM image of a 10-layer copolymer LB film sample.

AFM result

Figure 6 presents the topographic images of the quartz glass surface coated with PDPA-*b*-PDMA-*b*-PDPA triblock copolymer molecules. The scale was set in such a way that light colors correspond to higher structures. The morphological examination of the copolymer LB film was carried out using AFM in the dynamic mode. Figure 6 depicts 5 × 5 µm areas of three-dimensional AFM image of a 10-layer copolymer LB film deposited at a rate of 25 mm min^{-1} onto a flat quartz glass substrate. The AFM analysis indicate that 10 layers of the copolymer LB thin films are homogeneously deposited with average roughness (R_a) of 0.60 nm and a root-mean-square roughness (R_q) of 0.84 nm on a 5 × 5 µm scale. However, the AFM image of the copolymer LB sample consists of grainy structures in certain areas with the height of the highest peaks (R_p) of 16.26 nm. The reason behind the high value of R_p is that molecular clusters with long chains of copolymer molecules are formed during the formation of thin films, resulting in the formation of high hills in certain areas. On the other hand, this morphology has proved to be very useful for gas sensing, in order to promote ingress and egress of the VOCs into and from the thin film.

Sensing properties of the copolymer LB film

Figure 7 shows the kinetic response for the 10-layer copolymer LB films against the saturated organic vapors. In Fig. 7, the frequency shift was monitored as a function of time during

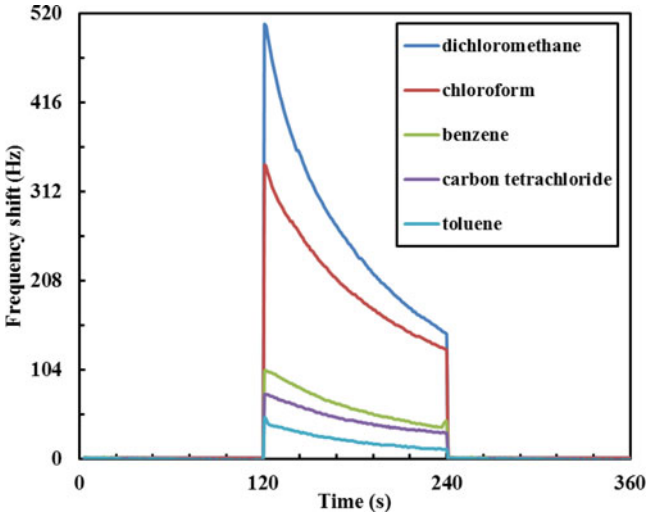

Figure 7. The frequency change of the copolymer LB film against organic vapors.

periodic exposure of the copolymer LB film sensor to several organic vapors (dichloromethane, chloroform, benzene, carbontetrachloride, and toluene) for 2 min, followed by the injection of dry air for another 2 min period.

In the initial step, the copolymer LB film sensor was exposed to fresh air for 120 sec, and a stable value was obtained as a response. In the second step, the first response of Langmuir-Blodgett film sensor to organic vapors carried out between 120 and 125 sec because of the surface adsorption effect between Langmuir-Blodgett film sensor and organic vapors. After this interaction, the bulk diffusion process caused an increase in effective mass, which reduced the response of the Langmuir-Blodgett film sensor, in direct proportion to the VOCs' pressure. The frequency shifted as function of the number of adsorbed VOC molecules. In the third step (in the 240 sec), after the fresh air was injected by syringe into the sensing chamber, the gas molecules adsorbed to the surface of the thin film were quickly separated from the surface. Therefore, a rapid decrease on sensor response occurred between 240 and 244 sec while the adsorption continued. In the last step, after 245 sec, the response of thin film sensor attained an initial baseline. QCM kinetic measurement was carried out for three cycles to observe reproducibility of sensor material. These three cycles of kinetic measurement indicated that the sensor response is reproducible for all organic vapors used in this study.

In Fig. 8, the kinetic vapor response of the copolymer LB thin films in exposure to different concentrations of VOCs' vapors (dichloromethane and chloroform) is given in terms of the change in resonance frequency over time. The VOCs' vapor was injected into the gas cell for 2 min at diluted amounts of saturated vapor concentration followed by 2 min recovery with dry air. The concentrations of VOCs' vapor (saturated gas diluted with dry air) used were 20%, 40%, 60%, 80%, and 100%. The decrease in resonance frequency of the quartz crystal resonator is proportional to the increase in mass due to presence of vapor adsorbed on its surface. All copolymer LB thin films give fast response to the VOCs' vapor in the range of a few seconds. The thin films recover themselves to their initial values after they are flushed with dry air, which means that they can be used multiple times.

The frequency shifts of copolymer LB thin film sensor versus the volumes of the two VOCs are plotted and shown in Fig. 9. After each injection of VOCs, the adsorption of VOCs onto the LB thin films results in a decrease in the resonance frequency of the quartz crystals. It is

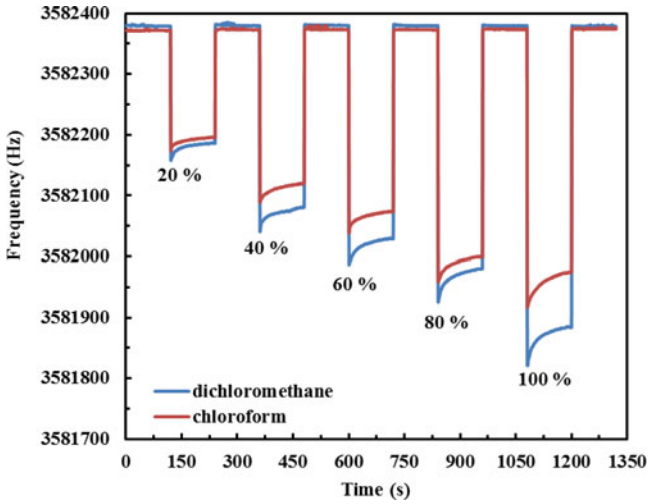

Figure 8. The response of copolymer LB sensor to different concentrations.

found that with the enhancement of gas volume, the frequency shift increases and gives an almost linear response to gas volume for dichloromethane and chloroform. The concentration values of organic vapor (seen in Table 1) in ppm can be calculated by the following formula: [20]

$$c = \left[(\rho V/M) \times 10^6\right] / \left[V_0/(24.055L/mol)\right] \tag{3}$$

$$c = [24.055\rho V/MV_0] \times 10^6 \tag{4}$$

where, c (ppm) is the concentration of VOC vapor, ρ (g/mL) is the density of VOC, V (mL) is the volume of VOC vapor that is injected into the gas chamber, M (g/mol) is the VOC molecular weight, and V_0 is the volume of the gas chamber (i.e., ~ 0.02 L). The vapor volume values used in this study are 20% for $V = 2$ mL, 40% for $V = 4$ mL, 60% for $V = 6$ mL, 80% for $V = 8$ mL, and 100% for $V = 10$ mL.

The limit of detection (LOD) of the copolymer LB film sensor was calculated by the measured sensor sensitivity (Hz per ppm). LOD is defined by [21]

$$LOD = 3\sigma/S, \tag{5}$$

where σ is the noise level of the fabricated QCM sensor, and S is the sensitivity to a specific analyte of the sensor. The sensitivity of LB film sensor was obtained from the frequency shift curves when exposed to organic vapors in Fig. 9. The approximate values of the curves were obtained from this figure. In this study, the resonance frequency was recorded in air for use as the absolute frequency of the QCM system, and the frequency response was stable within ±2 Hz over a period of 30–45 min. Therefore, the frequency noise was estimated at 2 Hz. The sensitivity and detection performance of the fabricated QCM sensor to several volatile organic vapors is given in Table 2. The copolymer-coated QCM sensor displayed sensitivity with detection limits of 28.21 and 30.72 ppm for dichloromethane and chloroform organic vapors at room temperature, respectively.

When Fick's second law of diffusion is applied to a plane sheet and solved by assuming a constant diffusion coefficient, the following Equation is obtained for concentration changes

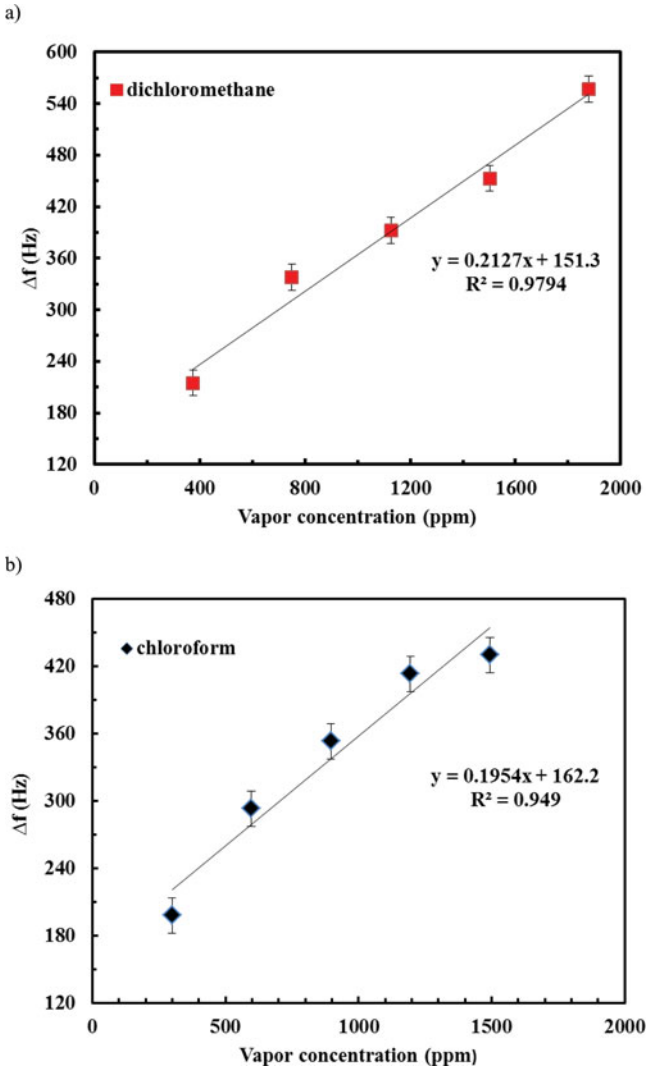

Figure 9. Frequency shifts versus concentrations of (a) dichloromethane, and (b) chloroform vapors.

in time [22]:

$$\frac{C}{C_0} = \frac{x}{d} + \frac{2}{\pi}\sum_{n=1}^{\infty}\frac{\cos n\pi}{n}\sin\frac{n\pi x}{d}\exp(-\frac{Dn^2\pi^2}{d^2}t), \tag{6}$$

where d is the thickness of the slab, D is the diffusion coefficient, and C_0 and C are the concentration of the diffusant at time zero and t, respectively. x corresponds to the distance at which C is measured. We can replace the concentration terms directly with the amount of diffusant by using

$$M = \int_V CdV, \tag{7}$$

where M is the mass uptake and V is the volume element. When Equation (1) is considered for a plane volume element and substituted in Equation (7), the following solution is

Table 1. The concentration values of organic vapors.

Organic vapors	ρ (g/cm^3)	M (g/mol)	c (20%) ppm; c (40%) ppm; c (60%) ppm; c (80%) ppm; c (100%) ppm
Dichloromethane	1.326	84.93	375.56; 751.13; 1126.70; 1502.26; 1877.83
Chloroform	1.483	119.38	298.82; 597.64; 896.47; 1195.29; 1494.11

Table 2. Sensitivity ot the copolymer QCM sensor to different chemical vapors.

Organic vapors	Sensitivity (Hz/ppm)	Detection limit (ppm)
Dichloromethane	0.2127	28.21
Chloroform	0.1954	30.72

obtained [23]:

$$\frac{M_t}{M_\infty} = 1 - \frac{8}{\pi^2}\sum_{n=0}^{\infty}\frac{1}{(2n+1)^2}\exp(-\frac{(2n+1)^2 D\pi^2}{d^2}t), \tag{8}$$

where M_t penetrant mass sorbed into the deposited film, assuming a one-dimensional geometry. The quantity, M_∞, represents the amount sorbed at equilibrium; t is the time. This Equation can be reduced to a simplified form

$$\frac{M_t}{M_\infty} = 4\sqrt{\frac{D}{\pi d^2}}t^{1/2}, \tag{9}$$

which is called early-time equation, and this square root relation can be used to interpret the swelling data [24].

To measure the kinetic data given in Fig. 7, it is required to take the copolymer LB film parameters because of swelling. Figure 10 represents the normalized frequency change against swelling time where the consolidation process involves setting starting times to $t = 0$ for each

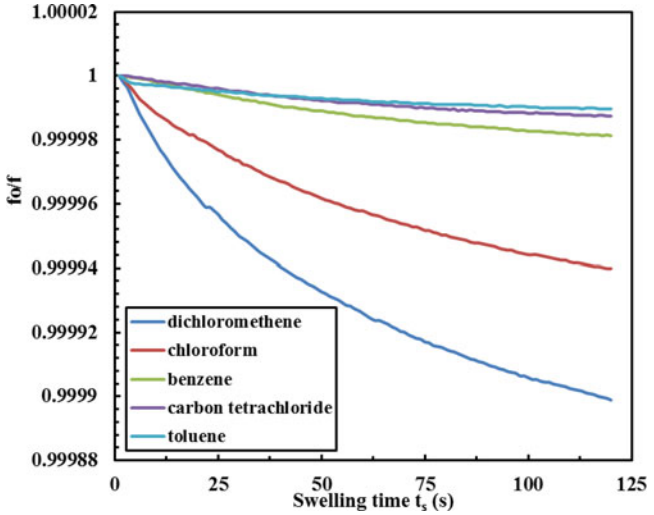

Figure 10. Normalized frequency changes against swelling time, t_s, for organic vapors.

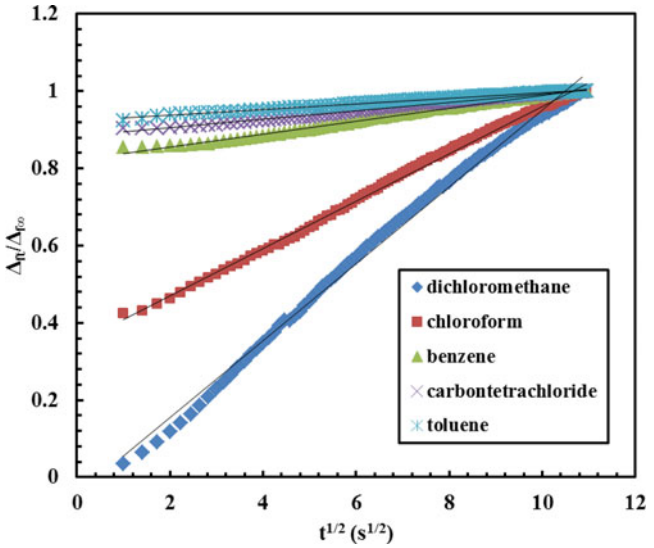

Figure 11. Plot of the normalized frequency against square root of swelling time, t_s. The solid line represents the fit of the data to Equation (10).

swelling cycles. It can be seen that changes in the normalized frequency against the time of vapor exposure decreased very fast as the saturated vapor injected into the gas cell is increased. These behaviors can be declared with the chain interdiffusion between copolymer chains during vapor exposure. As the saturated vapors penetrate into copolymeric film, the copolymer chains interdiffuse, which results in the decrease of the normalized frequency from the copolymeric film. These results can be related to the amounts of diffusant entering the copolymeric film M_t; that is, Δ_{ft} should be directly proportional to M_t [22]. Equation (9) now can be written as

$$\left(\frac{M_t}{M_\infty}\right) \approx \left(\frac{\Delta f_t}{\Delta f_\infty}\right) = 4\sqrt{\frac{D}{\pi d^2}}t^{1/2}, \tag{10}$$

where Δ_{ft} and $\Delta_{f\infty}$ are the normalized frequency shift at any time t and saturation point in Δ_f, respectively. The normalized Δ_f values $[\Delta_{ft}/\Delta_{f\infty}]$ are plotted in Fig. 11 for the square root of swelling time according to Equation (10). The slopes of the linear relations in Fig. 11 found the diffusion coefficients, D_s, for the swelling of copolymeric film.

As shown in Fig. 7, the resonance frequency changes of the copolymer thin film sensor for the organic vapors are, apparently, in the following order: dichloromethane > chloroform > benzene > carbontetrachloride > toluene. A similar result was found for diffusion coefficients as 39.90×10^{-16}, 15.14×10^{-16}, 1.12×10^{-16}, 0.79×10^{-16}, and 0.48×10^{-16} $cm^2\ s^{-1}$ for organic vapors, respectively. The interaction of these gases with the LB thin films is believed to be a physical absorption through a dipole–dipole interaction or hydrogen bonding [25]. The high values of diffusion coefficient obtained for chlorinated aliphatic hydrocarbons especially for dichloromethane and chloroform compared with other organic vapors. This may be explained by the high dipole moment values of dichloromethane (1.60 D) and chloroform (1.04 D), which explains this effect as previously been reported by other research groups [26, 27]. The relatively lower response was observed for toluene (0.60 D), carbontetrachloride (0 D), and benzene (0 D). However, the sensitivity of the copolymer film sensor against toluene vapor is slower than carbontetrachloride and benzene vapors. This can be clarified

with the fact that the molar volume of toluene (107.00 cm^3 mol^{-1}) is bigger than the carbontetrachloride (97.10 cm^3 mol^{-1}) and benzene (86.36 cm^3 mol^{-1}). While toluene molecule can difficultly diffuse into the copolymer thin films, the penetration of carbontetrachloride of benzene molecules into the same thin films is faster.

Conclusion

In this study, the PDPA-*b*-PDMA-*b*-PDPA triblock copolymer was synthesized, characterized, and investigated for its gas sensing properties using NMR, UV-vis spectroscopy, AFM, and QCM techniques. PDPA-*b*-PDMA-*b*-PDPA triblock copolymer LB film transfer on the solid substrate has been found to be successful with a high transfer ratio of ~92%. Also, a linear relationship between the number of layer and the absorbance shift shows that the PDPA-*b*-PDMA-*b*-PDPA triblock copolymer molecules are deposited orderly onto solid substrates. Similar linear relationships that were obtained with respect to deposited mass onto quartz crystal substrate was observed for resonant frequencies versus layer number. The typical Δ_f per layer was 286.15 Hz per layer and the deposited mass onto quartz crystal was calculated as 3893.15 ng per layer (14.69 ng mm^{-2}). The sensitivities of the copolymer-coated QCM sensor against organic vapors are obtained for dichloromethane and chloroform as 0.2127 and 0.1954 Hz ppm^{-1}, respectively. This sensor displayed sensitivity with detection limits of 28.21 and 30.72 ppm for dichloromethane and chloroform organic vapors at room temperature, respectively. Diffusion coefficients are found to be 39.90×10^{-16}, 15.14×10^{-16}, 1.12×10^{-16}, 0.79×10^{-16}, and 0.48×10^{-16} cm^2 s^{-1} for dichloromethane, chloroform, benzene, carbontetrachloride, and toluene, respectively. QCM results show that the response to chlorinated aliphatic hydrocarbons (dichloromethane and chloroform vapors) is higher than that of the other organic vapors used in this work. These results can be clarified with the dipole moment and molar volume of organic vapors. The response has been attributed to dipole–dipole interaction or hydrogen bonding between the thin films and the gas molecules. The PDPA-*b*-PDMA-*b*-PDPA triblock copolymer material can be used as a sensing material and may find potential applications in the development of room temperature organic vapor sensing devices.

Funding

This work was financially supported by The Research Foundation of Usak University (BAP) under project number 2014/MF014 and the Scientific and Technological Research Council of Turkey (TÜBİTAK) under project number 113Z584.

References

[1] Vasiukov, D., Panier, S., & Hachemi, A. (2015). *Int. J. Fatigue*, *70*, 289.
[2] Sedláček, O., Kučka, J., & Hrubý, M. (2015). *Appl. Radiat. Isotopes*, *95*, 129.
[3] Cantu, M. L., Chafiq, A., Faissat, J., Valls, I. G., & Yu, Y. (2011). *Sol. Energ. Mat. Sol.C*, *95*, 1362.
[4] Bousquet, A., Awada, H., Hiorns, R. C., Lartigau, C. D., & Billon, L. (2014). *Prog. Polym. Sci.*, *39*, 1847.
[5] Maute, M., Raible, S., Prins, F. E., Kern, D.P., Ulmer, H., Weimar, U., & Göpel, W. (1999). *Sens. Actuators B*, *58*, 505.
[6] Mondal, H. H., & Mukherjee, M. (2012). *Polymer*, *53*, 5170.
[7] Bosch, P., Fernandez, A., Salvador, E. F., Corrales, T., Catalina, F., & Peinado, C. (2005). *Polymer*, *46*, 12200.

[8] Spadavecchia J., Ciccarella, G., Valli, L., & Rella. R. (2006). *Sens. Actuators, B: Chem.*, *113*, 516.
[9] Edmiston, P. L., Campbell, D. P., Gottfried, D. S., Baughman, J., & Timmers, M. M. (2010). *Sens. Actuators B.*, *143*, 574.
[10] Hassan, A. K., Nabok, A. V., Ray, A. K., & Kiousis, G. (2002). *Mater. Sci. Eng. C*, *22*, 197.
[11] Homola, J. (2008). *J. Chem. Rev.*, *108*(2), 462.
[12] Kumar, A., Brunet, J., Varenne, C., Ndiaye, A., Pauly, A., Penza, M., & Alvisi, M. (2015). *Sens. Actuators B*, *210*, 398.
[13] Acikbas, Y., Erdogan, M., Capan, R., & Yukruk, F. (2015). *Res. Eng. Struct. Mat.*, *2*, 99.
[14] Açıkbaş, Y., Evyapan, M., Ceyhan, T., Çapan, R., & Bekaroglu, Ö. (2009). *Sens. Actuators B*, *135*, 426.
[15] Taktak, F., & Bütün, V. (2010). *Polymer*, *51*(16), 3618.
[16] Hussain, S. A., Dey, D., Chakraborty, S., & Bhattacharjee, D. (2011). *J. Lumin.*, *131*, 1655.
[17] Xu, W., Li, T., Li, G., Wu, Y., & Miyashita, T. (2011). *J. Photochem. Photobiol. A*, *219*, 50.
[18] Sauerbrey, G. Z. (1959). *Z. Phys.*, *155*, 206.
[19] Li, T., Mitsuishi, M., & Miyashita, T. (2001). *Thin Solid Films*, *389*, 267.
[20] Fan, X., & Du, B. (2012). *Sens. Actuators B*, *166–167*, 753.
[21] Sun, P., Jiang, Y., Xie, G., Yu, J., Du, X., & Hu, J. (2010). *J. Appl. Polym. Sci. 116*, 562.
[22] Erdogan, M., Capan, R., & Davis, F. (2010). *Sens. Actuators B*, *145*, 66.
[23] Crank, J. (1970). *The Mathematics of Diffusion*, Oxford University Press: London.
[24] Erdogan, M., Capan, I., Tarimci, C., & Hassan, A. K. (2008). *J. Colloid Interf. Sci.*, *323*, 235.
[25] Çapan, İ., & İlhan, B. (2015). *J. Optoelectron. Adv. Mater.*, *17*, 456.
[26] Ichinohe, S., Tanaka, H., & Kanno, Y. (2007). *Sens. Actuators B*, *123*, 306.
[27] Ceyhan, T., Altındal, A., Özkaya, A. R., Erbil, M. K., & Bekaroğlu, Ö. (2007). *Polyhedron*, *26*, 73.